

Automatic leaf segmentation and overlapping leaf separation using stereo vision

Zainab Mohammed Amean ^{b,a,*}, Tobias Low ^{a,c}, Nigel Hancock ^{a,c}

^a University of Southern Queensland, Toowoomba, Queensland, Australia

^b Control and Systems Engineering Department, University of Technology, Iraq

^c Centre for Agriculture Engineering, University of Southern Queensland, Toowoomba, Queensland, Australia

ARTICLE INFO

Keywords:

Machine vision
Stereo vision
Depth segmentation
Crop monitoring
Leaves detection
Overlapping leaves

ABSTRACT

Farm management and crop quality assessment is becoming increasingly automated to keep up with demand. The physical examination of the plant leaves, stems and fruit can provide valuable information about a plant's health. Automating the visual inspection through machine vision spawns challenges such as occlusions, irregular lightning and varying environmental conditions. In this paper, a plant leaf extraction algorithm utilising depth from a stereo vision sensor is presented. The algorithm tackles multiple leaf segmentation and overlapping leaf separation through synergising features such as colour, shape and depth. Depth is particularly used to measure discontinuities along its gradient in the disparity maps. The algorithm has a segmentation rate of 78% for individual plant leaves, over a range of complex backgrounds and changing plant canopies. The proposed algorithm was evaluated using 272 cotton and hibiscus plant images with results demonstrating that depth properties were effective in separating occluded and overlapping leaves, with a high separation rate of 84%. Leaf occlusion could be detected automatically without adding any artificial tags on the leaf boundaries. Furthermore, the results show a nearly identical performance for both types of plants (cotton and hibiscus) under various lighting and environmental conditions. The developed algorithm could be potentially applied to other types of plants that have similar structures to cotton and hibiscus.

1. Introduction

Plants typically display a variety of visual parameters which reflect their stress and survival requirements. The automatic detection of individual leaves is an essential task for precision applications in agriculture, which could benefit the implementation of many field practices and crop management strategies. The detection of multiple plant leaves on a growing plant under natural conditions is a crucial and challenging task for vision-guided agriculture robots [1]. This is due to many reasons, including colour similarities between a leaf and background foliage, similar characteristics of leaves on the same plant, plant structure complexity, leaf occlusion and the exhibition of different leaf size in the image.

There are numerous machine vision studies concerned with the analysis of two-dimensional (2D) image features, such as colour, shape, and texture, to address some of the problems in precision agriculture, ranging from weed control [2–4] to crop estimation [5–7], disease detection [8–14] and automatic monitoring of plants [15,16]. However, the detection of these image features depends on the growth stage, season, ambient conditions, and image acquisition [17]. Furthermore, most of the research tend to deal with a simple plant structure

(small seedling) [18] at an early growth stage or large-scale analysis (weed) [3].

The image analysis techniques used for identifying individual leaves depend on variety of factors. For example, the position (e.g. from the top or side view) from which the camera takes the images can capture a variety of different leaf orientations (horizontal or vertical) and change whether leaves are occluded or not. Top-view images usually offer a horizontal orientation for plant leaves which are completely visible or partially occluded, while variety of leaf orientations can be seen from side-view images. Most studies dealing with multiple leaf detection techniques are concerned with top-view images of small seedlings or non-complex plant canopies using different 2D imaging techniques [1, 18–24]. In addition, a variety of machine learning approaches have been also used to identify multiple leaves in plant images. For example, genetic algorithms [25] and neural network techniques [26,27] have demonstrated high performance in extracting individual leaves from canopy images and detecting vegetation pixels from the ground, respectively. The use of watershed-based leaf segmentation algorithms for

* Corresponding author at: Control and Systems Engineering Department, University of Technology, Iraq.
E-mail address: Zainab.S.MohammedAmean@uotechnology.edu.iq (Z. Mohammed Amean).

extracting plant leaves from foliage images was also reported in [28–32]. The methods reported above show an efficient segmentation of plant leaves from their background. However, their segmentation was not based on identifying connected leaves or handle occlusions.

Some studies have considered individual leaf segmentation and to handle the overlapping leaves problem for top view images using various shape techniques [33–35], 3D histogram segmentation technique [36] and neural networks technique (CNNs) [37]. Other studies used leaf shape features to perform leaf segmentation and to deal with the detection of partially occluded plant leaves [1,19]. These studies reported that shape traits provide a distinct feature that can aid in identifying partially occluded leaves. Although satisfactory segmentation rates were observed, shape feature is inadequate for irregular and complicated leaf shapes, or dense plant canopies. Furthermore, the prior knowledge of leaf shape in these studies introduces a potential limitation when attempting segmentation for plants with different leaf shapes. Furthermore, 2D images based segmentation are vulnerable to the complicated environmental factors. If series occlusion appears in the image, 2D segmentation methods are prone to failures. Thus, satisfactory results were reported for this type of segmentation for standard plants and on several rosette plants.

Three-dimensional (3D) imaging technology has been introduced for its ability to add another feature, specifically depth, to analyse the 3D properties of plants to counteract problems with 2D features. This technology is widely used for plant part detection, reconstructing a 3D model of the plant canopy and for plant phenotyping analysis techniques under indoor conditions [38–48].

Various studies were developed utilising 2D or 2.5D sensors for identifying the occluded and non-occluded leaves [49]. Most of these studies intend to reconstruct 3D models of plants from 2.5D sensors that capture dense depth data such as stereo vision [47,50], time-of flight (ToF) camera [51] and RGB-D sensors like both versions of Microsoft kinect sensor (v1 and v2) [44,50,52]. A comparison between stereo vision and ToF for monitoring plant leaves show that, ToF sensor has low resolution, is more robust to object texture and better at extracting the leaf shape. On the other hand, stereo vision sensor has a higher resolution than the ToF and it is more robust to different lighting condition (sunlight) which preserved edge discontinuity [53].

[44] used Kinect v1 sensor for in situ individual leaf segmentation and to handle leaves occlusion focused on a single plant type in a controlled greenhouse lighting setting. [50] proposed a filter based method for segmenting overlapping leaves from 2.5D point cloud data at controlled light conditions. The method achieved high segmentation rate however, there are some limitations related to complexity of shape based detection method and cannot work under direct sun light conditions. [54] combined Region Based Convolutional Neural Networks (R-CNN) with Density-Based Spatial Clustering of Applications with Noise (DBSCAN) clustering algorithms to segment overlapped leaves. Recently, [52] prepared a portable device using Kinect v2 to capture a single viewpoint 2.5D frame of plant foliage for non-destructive and in situ leaf area measurement. Based on the reported results, the device can measures the surface area of non-occluded leaves but has some constraints working under direct sunlight at higher intensity lux range, and to identifying occluded leaves from series occlusion. This is due to the limited resolution of Kinect v2 in daylight where small physical separations between individual leaves cannot be captured [52].

It is also possible to reconstruct a 3D model of a plant from different viewframe of 2D sensors using two methods. First, the images are captured from different viewpoints by moving a single colour camera around the plant. Then, a special software called structure-from-motion (SfM) is applied to reconstruct the 3D model of a plant. For example, [55] and [50] used SfM method to generates 3D point cloud from multiple viewpoint of an object and then to reconstruct a 3D model of plant leaves. Later, [56] combined 2D and 3D segmentation techniques to automatically segment plant leaves from 3D images and then each segmented leaf is projected onto 2D images, and the watershed

algorithm is employed to handle leaves overlapping. These methods require manual manoeuvring of the camera around the target subject to generate the 3D model of the plant. Moreover, it is hard to apply them for outdoor applications at uncontrolled lighting conditions.

Second, a single camera setup and turntable for the plant or fixed rigs such as multi-camera setup. Two examples of this method are, multi-view stereo (MVS) [45] and shape-from-silhouette [57]. The reported results show shape-from-silhouette method was faster than other 3D reconstruction method, while MVS by [45] has high computational cost and hard to use in uncontrolled lighting conditions. The works cited above paid considerably less attention to occluded leaf segmentation of dense plant canopies under different outdoor illumination conditions. The results were limited to a greenhouse environment, indoor and outdoor (cloudy/shady) conditions using a variety of sensors. These sensors generate dense and an accurate 2.5D or 3D depth information, still there is a limit in there working specifications, [58]. Therefore, more challenges are expected for detecting leaves in outdoor (uncontrolled) environments and for mature plant canopies. Recently, stereo vision techniques have been successfully used for fruit harvesting in robot applications. They are expected to be equally beneficial for plant segmentation and identification, owing to the reliability of stereo vision sensors to generate depth data (disparity maps) and to work in outdoor environments under a variety of illumination conditions [59].

The above challenges provide the motivation to develop a stereo vision system which can be used on a robot platform to identify important plant features (e.g. leaves). This system can perform a variety of agricultural tasks, such as automatic monitoring of plant growth, disease inspection, and early indication of plant stress. The core contributions of this study over existing studies are summarised by the following key points:

1. Development of an image analysis algorithm that can segment a plant canopy from a non-simple background, under semi-structured outdoor environments and varying sunlight conditions (sunny, cloudy, and shady).
2. Development of a fully automated plant individual leaves segmentation and overlapping leaf separation algorithm by measuring the discontinuities along the gradient of depth in the disparity maps. This algorithm calculates the discontinuities along the gradient of depth values in a global manner and separate the overlapping items accordingly.
3. The proposed algorithm depends on stereo vision sensor images without adding any artificial tags on the leaves.

The machine vision system developed in this study can be applied to several commercial and scientific applications for the agricultural mobile robot. The stereo vision system used in this study (with the developed algorithms) can recognise the important features of plants (leaf) which can help monitor plants of different agriculture practices and identify certain problems related to plant growth and health, such as water stress, wilting, damage, and disease attack. This system can also analyse data, count the number of leaves, and find the position of each individual leaf in X , Y , Z coordinates. From this information, further information can be calculated such as plant height, width, and volume.

The remainder of this paper is organised as follows: Section 2 describes the methods and materials used in this study. Section 3 explains the proposed algorithm for plant leaf segmentation and overlapping leaf separation, and Section 4 presents the experimental results and discussion. Finally, a summary of the significant conclusions is presented in Section 5.

2. Materials and methods

2.1. Image acquisition

The 8-bit RGB colour Bumblebee2 stereo vision camera (designed by Point Grey Research Company, Canada) was adopted to capture colour

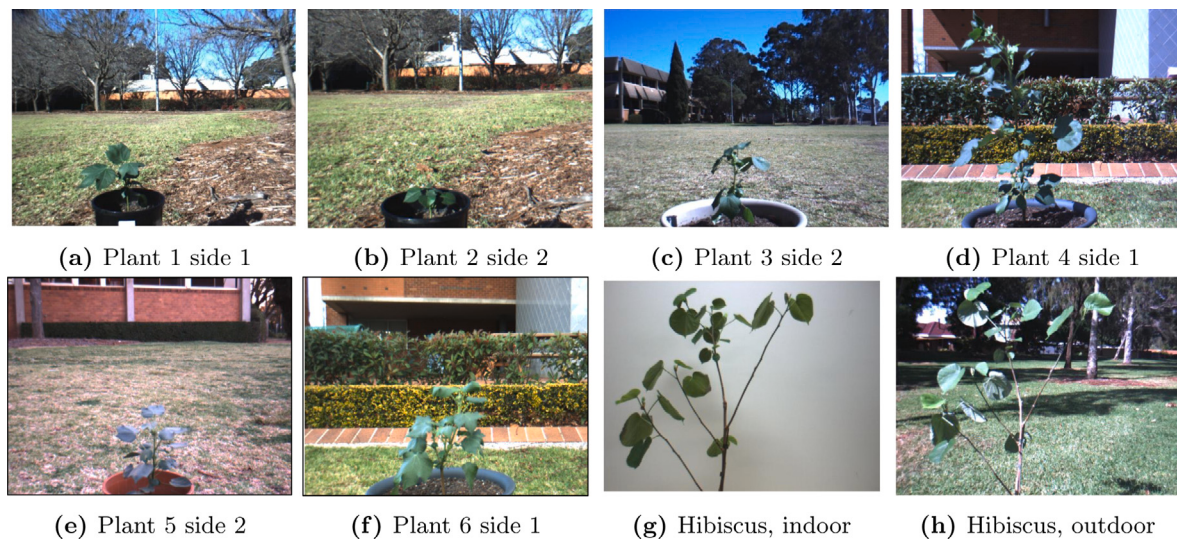


Fig. 1. Samples of cotton and hibiscus plants. (a)–(d) Cotton plants in sunny positions. (e) and (f) Cotton plants in shadow conditions. (g) and (h) Hibiscus plants in indoor (g) and outdoor (sunny) positions (h).

and depth images of plants. This stereo vision camera is powered by a 12 V Li-ion battery. The camera was chosen for its ability to produce disparity maps and work under outdoor conditions. It was installed on a tripod and connected to a laptop computer for capturing datasets of images. This packaged system has two digital charge-coupled device (CCD) cameras locked in a fixed assembly, which are pre-calibrated for both the stereo rig and lens distortion. The focal length (f) is equal for both cameras (2.5 mm), and they are separated by a 12 cm baseline (b) distance. The camera pixel resolution is 640×480 at 48 frames per second (FPS) or 1024×768 at 20 FPS. The Bumblebee2 camera produces raw colour images, left- and right-calibrated and rectified colour images, disparity images/maps, and 3D point cloud data. The Triclops software development kit (SDK) and FlyCapture application programming interface (API) functions were developed under Microsoft Visual C++ to capture the datasets of plant images with a resolution of 600×800 pixels.

2.2. Experimental plan and research focus

The experiments carried out in this study involve two types of plants (with different structures), namely cotton (*Gossypium hirsutum* L.) and hibiscus (*Hibiscus rosa-sinensis* L.) (Fig. 1). Hibiscus plants were studied initially for their clearly separated leaves, in progression, this research focused more on cotton plants for the following reasons.

Firstly, cotton plants absorb large amounts of water, as such, monitoring plant growth can significantly improve water usage. Secondly, cotton has perhaps the most complex growth habits, owing to the continuing vegetative growth after fruiting is initiated. Therefore, continuous monitoring of multiple plant features (vegetative growth, stem internode length, and fruit abscission), stress, and requirements can detect any imbalance in growth habits to improve management decisions. Lastly, there are no similar reported studies for cotton, and this research is expected to be applicable to other plants displaying a similar structure.

The cotton plants were planted in April 2014 in two different pot sizes, which resulted in two different growth rates; these were labelled as big cotton (350 mm pot diameter) and small cotton (250 mm pot diameter). Eight datasets of images were captured for different growth stages (two image sets for each growth stage) during the winter and early spring of 2014 in outdoor environments. Three main illumination conditions considered in this study were sunny (four datasets), shady (three datasets), and cloudy (one dataset). The images were captured from two labelled sides of the plant (to offer different leaf orientations)

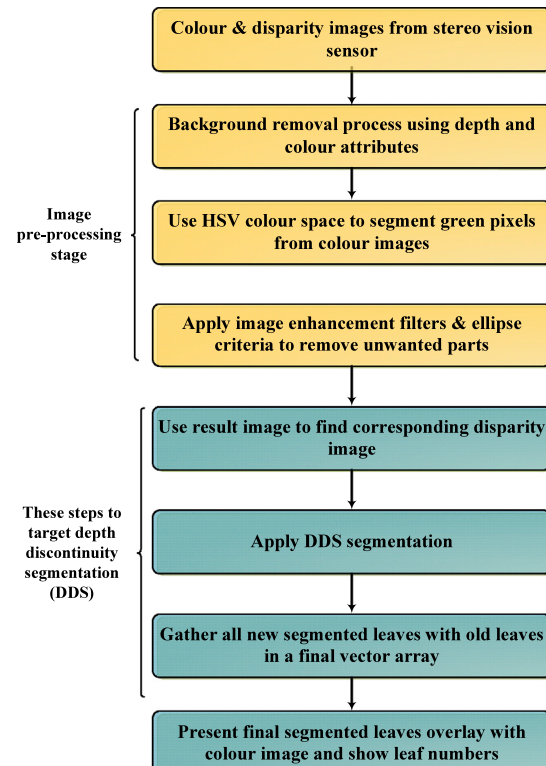


Fig. 2. Leaf segmentation and counting algorithm.

and from a distance between 0.85 and 1.25 m, depending on the plants' height and size. Images of the plants were taken on campus at a variety of locations, as shown in Fig. 1.

3. Leaf segmentation and counting algorithm design and methods

Fig. 2 describes the main steps of the newly developed segmentation algorithm, which consists of two stages: image pre-processing and enhancement techniques, and depth discontinuity segmentation (DDS) techniques. The first stage of the algorithm includes two steps:

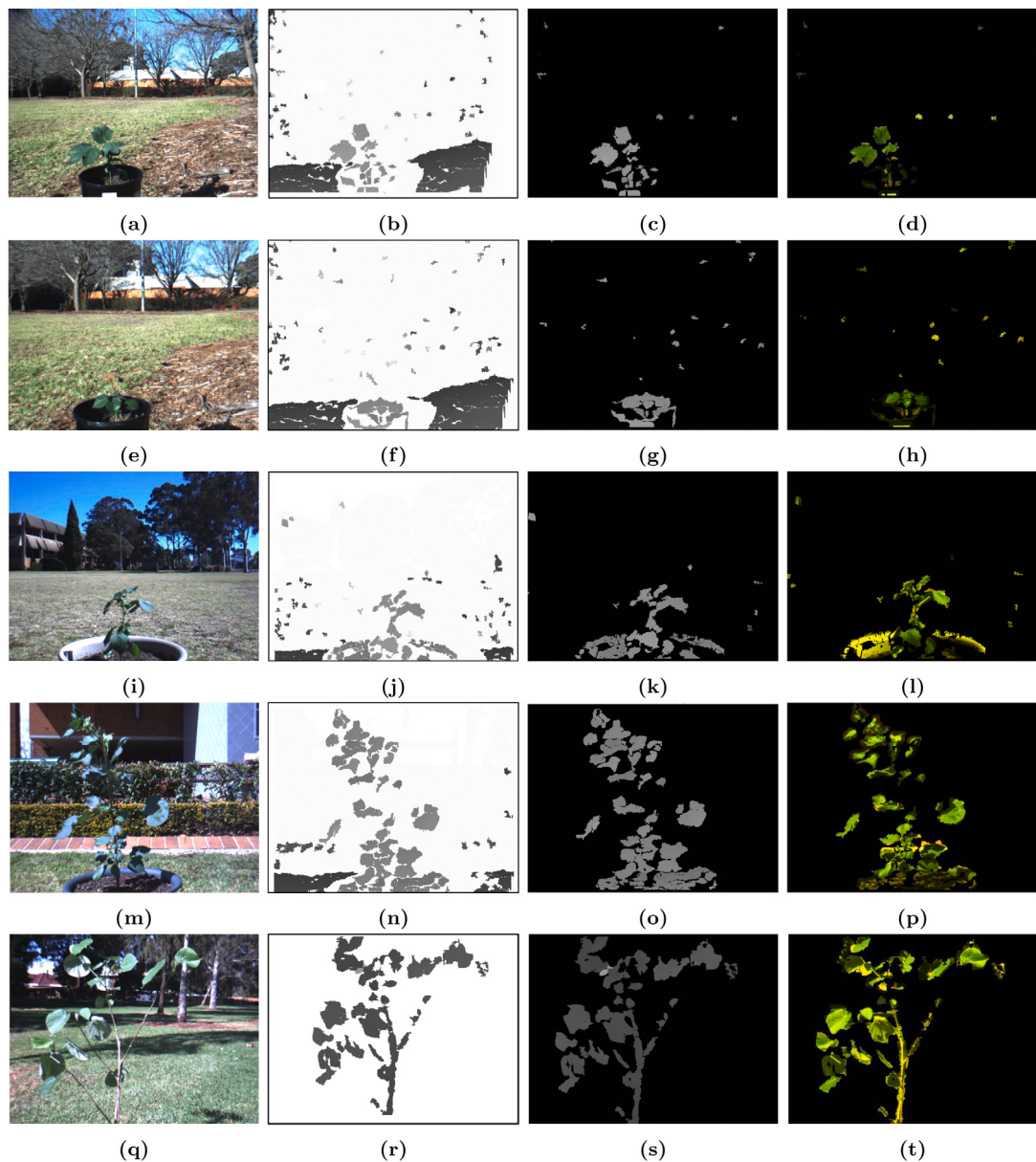


Fig. 3. Background removal process for the five selected cotton and hibiscus plant images. Column 1: colour images. Column 2: disparity maps. Column 3: filtered disparity maps. Column 4: colour images after depth mask for each of the R, G, and B colour channels. (For interpretation of the references to colour in this figure legend, the reader is referred to the web version of this article.)

Step1: Segmenting plant canopy (a cluster of leaves, stem and branches) from the background foliage.

Step2: Segmenting the cluster of leaves into the individual leaves and even smaller clusters where achievable by applying different segmentation techniques.

The resulting images from the first stage consists of plants with leaves being segmented individually and other still having connected or overlapped leaves in small clusters.

Initially, standard image processing techniques were applied to separate the overlapping leaves, such as erosion and dilation operators [60]. The output was far from the desired requirement for most leaves, owing to the working principles of both techniques. Therefore, their results were not considered. Some implications were:

1. Small leaves were removed by the erosion operator.
2. Other leaves were connected by the dilation operator.

Another segmentation method, named DDS, is developed based on depth discontinuity and gradient criteria. This method concerns with

leaf overlapping issues and benefits from depth information. Addressing other issues, such as eliminating the effects of the ambient illumination conditions on the segmented images, is beyond the scope of this study. The following sections address the new algorithm development procedures.

3.1. Image pre-processing method

The first stage of a plant segmentation algorithm is carried out using three segmentation steps: Background removal using colour and depth information; image segmentation based in hue distribution; and image enhancement and shape geometrical analysis. The following sections illustrates the algorithm steps and methodology.

3.1.1. Background removal process using depth and colour attributes

The detection of the plant regions of interest (ROIs) from the background was formulated using disparity maps as shown in Fig. 3, column 2. The quality of a disparity map depends on the setting of

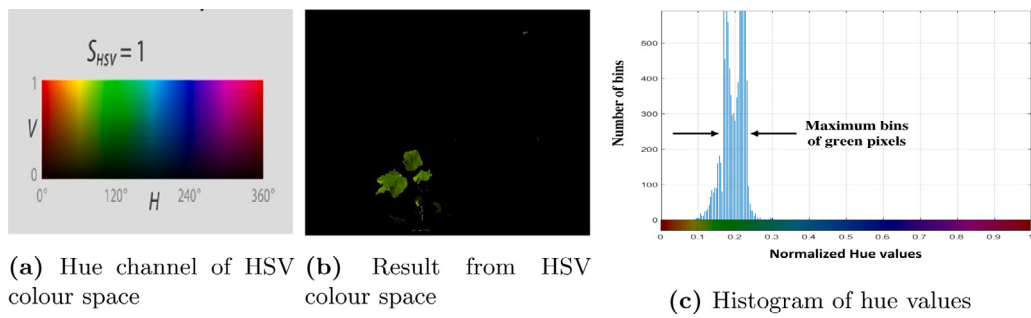


Fig. 4. HSV colour transformation for plant 1 side 1 of Fig. 1.

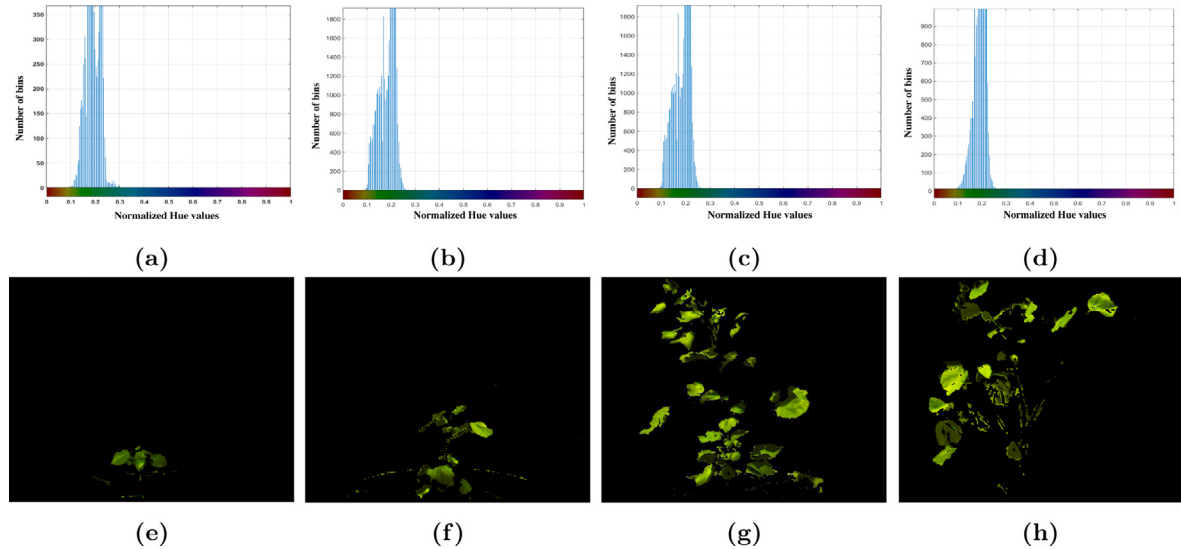


Fig. 5. Histogram distribution of the hue channel; result from HSV colour space transformation and applying the developed equations for the colour images of the other four selected cotton and hibiscus plants in Fig. 1. (For interpretation of the references to colour in this figure legend, the reader is referred to the web version of this article.)

the stereo and validation parameters. An optimal combination of these parameters was set that can fulfil the required criteria to produce in-depth information for plant parts, with a particular focus on leaves. More details about setting the stereo and validation parameters and the evaluating of the disparity maps are explained in [61]. This method intends to segment the foreground area from the background area by three steps:

1. A specific range of depth was assigned as a threshold value and used as a mask to segment the ROI from the original disparity map and produce a new disparity map, as presented in Fig. 3, column 3.
2. The colour images of plants in Fig. 1 were transformed to the R, G, and B colour channels.
3. The new disparity map was used as a mask for each R, G, and B channel to segment the colour image from the background. The ROI's were found, as shown in Fig. 3, column 4 which shows plant leaves, stem, branches, soil, and pot. Therefore, another segmentation technique based on colour was introduced to formulate the algorithm.

3.1.2. Image segmentation based on hue distribution

Leaves under outdoor conditions can exhibit different illuminations, which can result in different ranges of green colour. The hue, saturation, value (HSV) colour space transformation was used to segment green from the images since it is less affected by the ambient illumination and can retain the colour information (chromaticity) despite differences in luminance [62,63]. Therefore, only the hue channel was

used to capture the greenness of leaves under a variety of outdoor illumination phenomena, such as overexposure and shadow.

Fig. 4a presents the hue channel of the HSV colour space. Figs. 4c and 5 row 1 show a histogram of the normalised hue value distribution for plant 1, side 1 and the other four selected plants of Fig. 3 column 1. The scale of the hue distribution chart is normalised from 360 to 1. The maximum bins of the histogram distribution are within the range of green in the hue channel.

The mean (μ) and standard deviation (σ_h) values of the normalised hue distribution are determined. These values would vary from image to image depending on the histogram distribution of the hue. The calculated μ and σ_h are used to determine the upper and lower threshold values of the hue for green pixels using the developed equations, Eqs. (3.1) and (3.2).

$$LH = \begin{cases} \mu + \kappa_1 \times \sigma_h & \text{if } \mu \geq \tau. \\ \mu - \kappa_1 \times \sigma_h & \text{Otherwise.} \end{cases} \quad (3.1)$$

$$UH = \mu + \kappa_2 \times \sigma_h \quad (3.2)$$

where LH and UH are the upper and lower threshold values of the hue distribution for green pixels and κ_1 , κ_2 and τ are the initialisation parameters used to calibrate the equations. The initialisation parameters need to be adjusted only once for the algorithm. Prior to the initialisation of these parameters, the upper and the lower threshold values of multiple hue distributions of plant images selected randomly from different datasets were visually inspected and measured to find the range of green in the hue channel. From this measurement, it

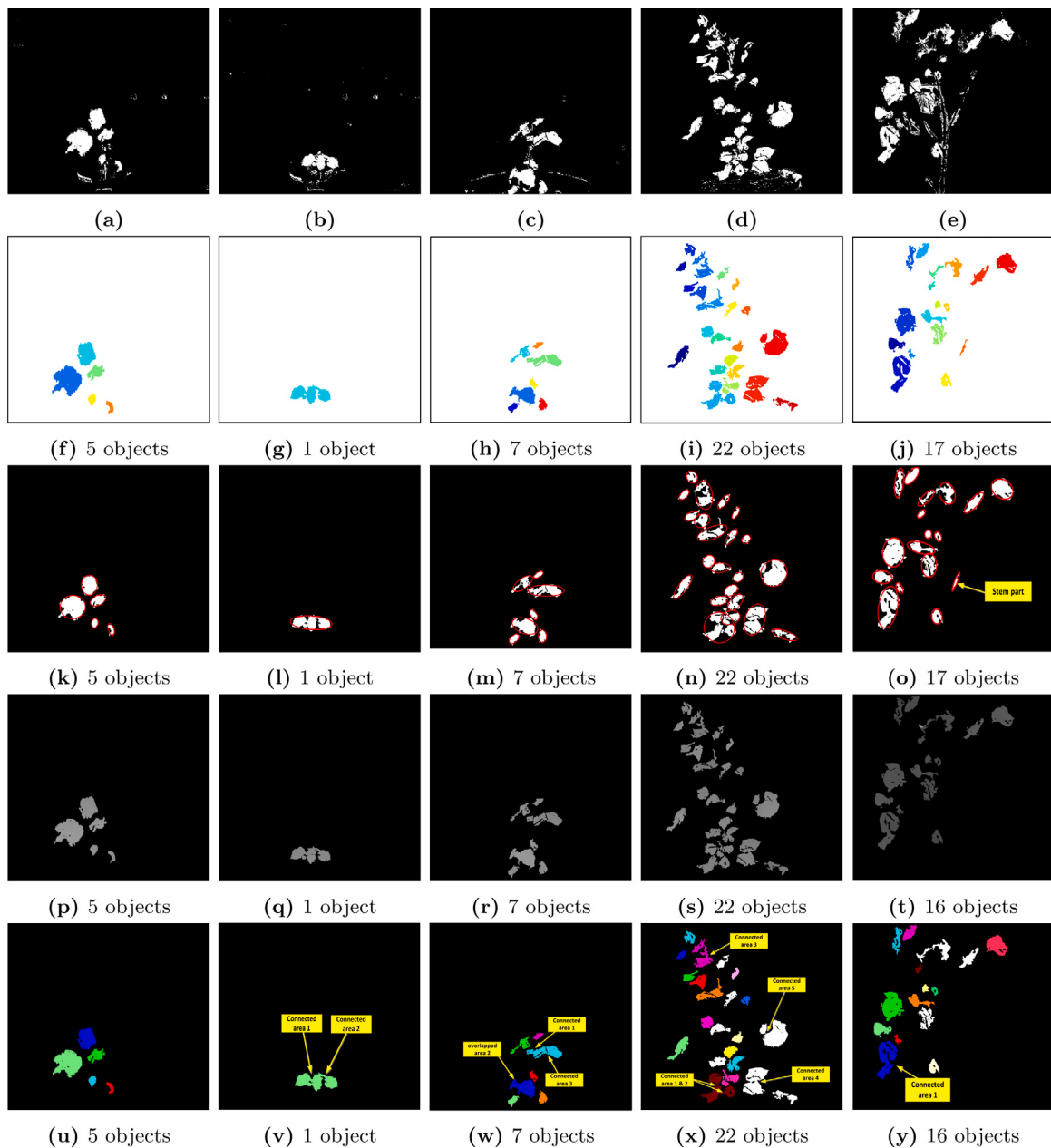


Fig. 6. Binary image transformation, image enhancement, and geometric shape analysis for the five selected cotton and hibiscus plants in Fig. 1. Row 1 = binary images result from hue channel. Row 2 = labelled leaves with different colours result from applying median filter and connected component algorithm. Row 3 = ellipse fitted to each leaf (red outline). Row 4 = equivalent disparity images after application of ellipse criteria. Row 5 = plant leaves segmented in different colours and overlying each other. (For interpretation of the references to colour in this figure legend, the reader is referred to the web version of this article.)

was observed that values of $\kappa_1 = 0.25$, $\kappa_2 = 3$, and $\tau = 0.19$ could effectively isolate foliage pixels, as shown in Fig. 5, row 2. The current setting of the parameters identifies only green objects. After the initial calibration of these parameters, the mean, standard deviation and the upper and lower threshold values were automatically calculated for each single plant image. Then, leaf pixels were isolated from those of other plant parts using the upper and lower threshold values of the hue distribution. Eqs. (3.1) and (3.2) were applied to eight sets of cotton plant images (252 images) under different illumination conditions and 20 images of hibiscus plants under indoor and outdoor conditions. The results show that the developed equations can reduce most of the elements of noise present in Fig. 5. Despite that, minor noise still exists in the green images of Fig. 5, row 2, and this is displayed more prominently in the binary image of Fig. 6, row 1.

3.1.3. Image enhancement and geometric shape analysis

Enhancement processes are implemented using different image processing techniques such as image filters, regions, and shape properties. A median filter, [64], of size (3×3) was applied owing to its capability to simultaneously reduce noise whilst maintaining image edges [65]. The connected component and labelling algorithm, also known as the ‘flood-fill algorithm’ [66], was applied to detect the connected regions in a binary image. The desired outcome is that each connected area corresponds to one object or one leaf. This algorithm can also filter images from noise and confirm leaf objects according to their size. A suitable threshold value was assigned to the algorithm according to the prior initialisation by inspecting multiple plant images selected randomly to discriminate between different leaf sizes. Accordingly, a 200 pixels threshold value revealed to be the optimal to retain plant leaves for early growth stages (i.e. datasets 1, 2, 3, and 4), and a

300 threshold for other growth stages (i.e. datasets 5, 6, 7, and 8). The objects below this threshold value were removed from the images. Fig. 6 represents the initial estimation of leaf numbers in the image after applying this algorithm and the median filter. Several images still have other objects such as portions of plant stems and branches or partially occluded and overlapped leaves, hence, further segmentation steps are required.

Leaf contours with elliptical shapes are the most common method currently used to extract the important features of leaves [67,68]. The geometric measurements such as the minor and major axes of the ellipse, or the axis ratio (slimness) [69] is beneficial for further analysis. Prior to the determination of these values, an ellipse was fitted to each object on the image as shown in Fig. 6, row 3. Then, the minor axis, major axis, and axis ratio for each object in the image were measured. Following this step, the measured values were saved and investigated to calculate the maximum values of major axis and axis ratios for all plant leaves used in this study to assign threshold values. These values, Th_1 and Th_2 , are used to discriminate between leaf and non-leaf objects using the following criteria:

$$\text{MajorAxis} \leq Th_1 \quad (3.3)$$

and,

$$\text{AxisRatio} = \frac{\text{MajorAxis}}{\text{MinorAxis}} \leq Th_2 \quad (3.4)$$

It was found that objects that have a major axis greater than 190 and axis ratio more than 5.5 form a tall and very thin object. Such an object cannot be a leaf object. It could be a part of a stem or branch, and therefore it was removed from the image. The two values were determined as threshold values for the developed criteria, specifically $Th_1 = 190$ and $Th_2 = 5.5$, and needed to be set only once as an initial calibration. These values work effectively for all data used in this study in all instances. Having said that, these values might not work with other types of plants with different leaf sizes (larger leaf sizes than cotton and hibiscus leaves), thus, a new calibration would be required. The binary image utilised to find the ellipse criteria was also used as a mask to find the corresponding pixels in the disparity image, as presented in Fig. 6, row 4.

Only one object was removed (a part of a stem) from hibiscus plant image as shown in Fig. 6, row 4. Fig. 6, row 5 shows plant leaves were segmented individually (most cases) and others are connected or overlapped in small clusters. These leaves are distinctly coloured and overlaid on each other (to perform the first stage of the segmentation). Only plant 1, side 1 (Fig. 6u) displays 100% segmentation accuracy. By visual inspection, the other sample plants have several leaves which are segmented incorrectly owing to the leaves touching or overlapping.

3.2. Depth discontinuity segmentation algorithm (DDS)

A segmentation method has been developed and presented to separate the overlapped leaves based on depth discontinuity criteria. A significant local change in image intensity can assign an edge in an image. The change is usually associated with a discontinuity in either the image intensity or its first derivative [70]. Accordingly, a discontinuity of pixel values can assign the existence of two or more leaves in the image. Therefore, some of the standard segmentation techniques such as edge finding correlation techniques were investigated by [71] and [72] to detect a discontinuity of pixel values and to solve overlapping issues. It was observed that these techniques provided distinct edges for leaf boundaries but they were unable to recognise the internal discontinuities in depth values within the overlapped leaves. These unrecognised values were examined, and the following findings were obtained:

The variance in depth intensity between two overlapping regions is not sufficiently distinctive to be recognised by edge detection techniques (also with low threshold settings) compared with the variance

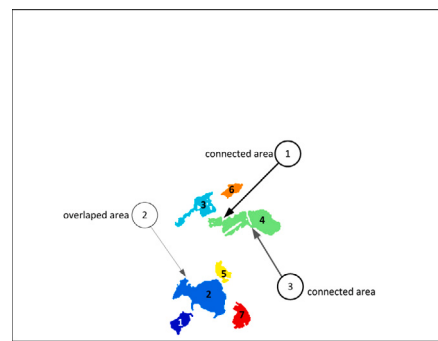


Fig. 7. Plant 3 side 2 colour segmentation showing connected areas 1 and 3 and overlapped area 2.

in depth intensity between leaves and the background. The smooth gradient in depth was assigned to one leaf in the image, whereas a depth gradient larger than three pixel values presented two different leaves.

The discontinuity in the depth values for the segmented leaves is measured by calculating the increment between the disparity map elements. Two different depth measurement methods (global and local) were developed in this study. Local measurement uses a direct comparison between each pixel and its neighbourhood. While the 'global measure' calculates the discontinuity in depth without the need to examine each pixel in the image. The new developed algorithm consists of four main techniques: disparity map denoising (DMD) as well as global and local discontinuity segmentation and zero neighbours counting (ZNC). The global measurement was applied first to consider the computation cost.

Plant 3 side 2 (Fig. 3i) was selected as an example to show the detailed process when applying these techniques. Commencing in connected area 1 of Fig. 7, the algorithm techniques were applied sequentially to each object, as in the following sections (Sections 3.2.1–3.2.4).

3.2.1. Disparity map denoising technique (DMD)

This technique can be considered as pre-processing step by filtering the noise pixels in the disparity map. Figs. 8a and 8b presents one example of the separation process for the connected area (area 1) of plant 3 side 2 (Fig. 1c) using the DMD technique. The values of pixels in the disparity map range from 138 to 140 (Figs. 8a and 8b) and they show two overlapped leaves. The values of these pixels are proportional to the depth values (largest values indicate most distant leaves) in the image. The pixels valued 0 present the blank area in the image. The pixels valued 1 are suspected to have incorrect values of depth. These pixels are considered to be noise pixels owing to the mismatching process errors. Such errors are caused by many possible reasons, such as overlapping, insufficient light, shadow or overexposure. The DMD technique was applied to change the value of noise pixels from 1 to 0, as shown in Fig. 8b. Fig. 8c shows another example for applying this technique. Subsequently, other DDS algorithm techniques were applied to formulate the connected leaves separation in the already separated leaves (light blue area) of Fig. 8b.

3.2.2. Global discontinuity segmentation technique (GDS)

The process of segmentation based on global discontinuity is initiated by measuring the depth gradient over the whole area of an examined image. A smooth increment in depth between neighbouring pixels (i.e. an increment of one or two pixels) in the disparity maps, indicates one small or medium leaf with a flat pose. A difference in depth equal to three pixels and more indicates the existence of two overlapped leaves of small or medium size, or one large leaf with distinct depths across different lobes.

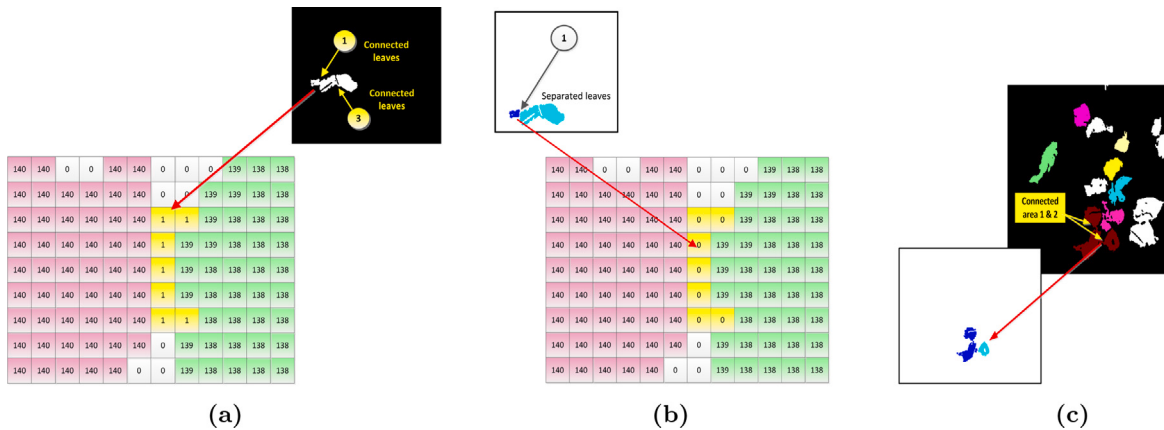


Fig. 8. Connected leaves of area 1 for plant 3. Leaves image and disparity map (a) before separation, (b) after separation. (c) Two connected areas of plant 4 side 1 separated using the DMD technique. (For interpretation of the references to colour in this figure legend, the reader is referred to the web version of this article.)

Fig. 9 shows distinct differences between neighbouring pixels ranging from 8 to 10 (shown as red versus green), indicating two leaves in the examined area. This indication was based on a threshold assigned by inspecting a wide range of disparity maps with overlapping and non-overlapping leaves. The depth gradient could be measured without the need to find the difference between each pair of contiguous pixels in the examined object. The global discontinuity segmentation (GDS) technique has been developed to benefit from the unique property by finding the unique pixels values in an array and generating the unique vector U . These values are sorted into ascending order and stored in the U vector (Eq. (3.5)). The difference between each pair of contiguous pixels of U is calculated. Then, the U vector is split into a group of smaller components, $U_1, U_2, U_3, \dots, U_m$ according to the difference value (i.e. difference value \geq threshold value (threshold ≥ 3)). The number of small components indicates the number of overlapping leaves, where each component contains only those disparity values corresponding to a single vector.

Fig. 9 and Eq. (3.6) show an example of two overlapping leaves which were successfully separated using the GDS technique. According to this technique, the Unique vector of these leaves is divided into two vectors U_1 and U_2 or two groups of pixels due to the difference between the contiguous pixels. Vector U_1 includes pixels of the red area and vector U_2 includes pixels of the green area. Each vector presents one leaf. This technique has an advantage over edge detection techniques by measuring the depth gradient discontinuity without the need to examine each pixel. However, both of them target the discontinuities of pixel values. In some cases, the unique vector indicates smooth increments in depth between its elements, while the colour image shows two overlapping leaves in this particular area. In this case, it is necessary to search for depth discontinuities using a local technique.

$$U = \begin{bmatrix} u_1 \\ u_2 \\ u_3 \\ u_4 \\ u_5 \\ u_6 \\ u_7 \\ u_8 \\ u_9 \\ \vdots \\ u_n \end{bmatrix} = U_1 \begin{bmatrix} u_1 \\ u_2 \\ u_3 \end{bmatrix} \| U_2 \begin{bmatrix} u_4 \\ u_5 \\ u_6 \end{bmatrix} \| U_3 \begin{bmatrix} u_7 \\ u_8 \end{bmatrix} \| \dots \| \dots U_m \begin{bmatrix} u_9 \\ \vdots \\ u_n \end{bmatrix} \quad (3.5)$$

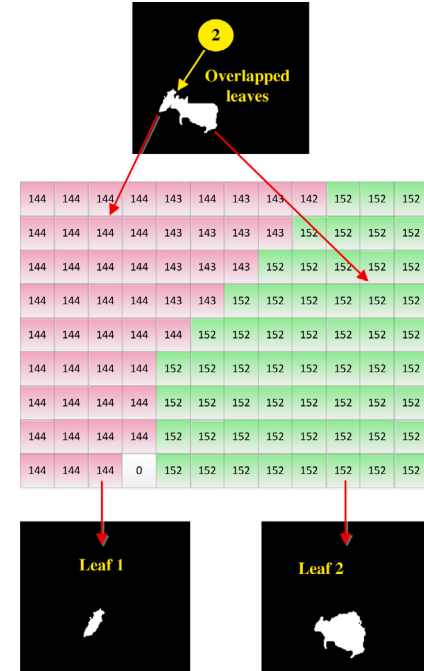


Fig. 9. Two overlapping leaves (area 2 of plant 3) and their separation process using the GDS technique. The top image shows the overlapping leaves. The disparity map declares the distinct difference between pixels. The lower images present the results after separation. (For interpretation of the references to colour in this figure legend, the reader is referred to the web version of this article.)

$$U = \begin{bmatrix} 142 \\ 143 \\ 144 \\ 145 \\ \dots \\ 148 \\ 149 \\ 150 \\ 151 \\ 152 \\ 153 \\ 154 \end{bmatrix} = U_1 \begin{bmatrix} 142 \\ 143 \\ 144 \end{bmatrix} \| U_2 \begin{bmatrix} 148 \\ 149 \\ 150 \\ 151 \\ 152 \\ 153 \\ 154 \end{bmatrix} \quad (3.6)$$

0	0	145	145	0	145	145	145	145	145	145	145
0	0	145	145	145	145	145	145	145	145	145	145
0	0	0	145	145	145	145	145	145	145	145	145
0	0	0	145	145	145	145	145	145	145	145	145
0	0	0	145	145	146	146	145	145	145	145	145
0	0	0	145	145	146	146	146	146	146	146	146
0	0	141	141	141	141	141	146	146	146	146	146
0	142	141	141	141	141	141	0	0	0	0	147
142	142	141	141	141	141	141	0	0	0	0	147
142	142	141	141	141	141	141	0	0	0	147	147

Fig. 10. Disparity map showing a big difference in neighbouring pixels when Eq. (3.7) indicates a smooth increment in unique vector U .

3.2.3. Local discontinuity segmentation: Eight neighbours difference technique (ENBD)

This technique was developed to separate those certain cases where the unique vector U (Eq. (3.5)) presents a smooth increment in depth between the elements of U . Contrary to that, the disparity map contains more than one leaf and a sharp gradient in depth was observed on the disparity map. A sharp gradient means that the difference between the neighbouring pixels exceeded threshold value. The ENBD is targeting those different areas based on the local discontinuity in depth. Fig. 10 and Eq. (3.7) illustrate an example of this case.

$$U = [141 \ 142 \ 143 \ 144 \ 145 \ 146 \ 147 \ 148] \quad (3.7)$$

Two ranges of pixels values (141 to 142) and (145 to 147) are presented by green and red areas respectively, (Fig. 10). As the difference between the neighbouring pixels is greater than the threshold, each area represents one leaf. The concept of this technique is to measure the difference in depth between the centre pixel and its neighbouring pixels using a convolution with a (3×3) kernel as shown in Figs. 11a-d. These figures represent the state of the matrix from an arbitrary start. The moving kernel calculates the absolute difference between the centre pixel (reference pixel) and the other eight neighbouring pixels. The process is formulated as follows:

The value of the neighbour pixel is set to zero when the absolute difference is greater than or equal to the threshold value. The neighbour pixel is skipped when the value of absolute difference is equal to zero meaning no change is made. The zero-valued centre pixels are also skipped and no change can be made because the absolute difference in depth between these pixels and any of the neighbouring pixels is equal to the values of the neighbouring pixel itself. Subsequently, the moving kernel completes the separation process for each column and shifts to the right progressively. The connected component and labelling algorithm (Section 3.1.3) was applied to verify the separation. All changed pixels are coloured red to declare their position after using the ENBD segmentation method (Fig. 11d).

3.2.4. Zero neighbours counting technique (ZNC)

The zero neighbours counting technique (ZNC) has been developed and applied in instances in which connected leaves did not separate after applying ENBD. These areas in the disparity map are still connected by a few pixels, because the difference in depth is less than the threshold value. Fig. 12a shows two leaves of plant 3 (area 3) connected by a small number of pixels, and illustrates the corresponding disparity map of the same two leaves.

The technique is formulated by moving a window of nine pixels over all pixels of the disparity map. The centre pixel is set as a reference pixel and its value is set to zero when the number of zero neighbours are three or more. This process is applied on all columns

and rows sequentially to accomplish leaves separation. Directly after the segmentation is confirmed and the separated leaves are labelled, the process stops and there is no need to examine all elements of the disparity map. The ZNC technique cannot be applied unless the discontinuity in depth is detected by the ENBD technique. Figs. 12b and 12c show the algorithm process. Figs. 13 demonstrate the operation of the ENBD and ZNC techniques to separate individual leaves. As per the labels in Figs. 13, some components were separated into individual leaves using only the ENBD technique (most cases) and others using both ENBD and ZNC techniques when necessary.

4. Results evaluation and discussion

The final plant leaf segmentations of the selected cotton and hibiscus plants of Fig. 1 are shown in Fig. 14. Columns two and four indicate the results have been improved by using the developed DDS and is recognised by the difference between the numbers of leaves in relevant columns. Table 1 confirms this incremental increase in accuracy from 72% to 91% as the proposed technique was added to the leaf segmentation algorithm. However, a minority of leaves are still missing from the final segmentation results due to the illumination condition issues and other factors that will be further explained with respect to different datasets in this section.

The evaluation of the algorithm was conducted on both cotton and hibiscus plant images to show its strength, ability to work under varied conditions, and address some current limitations in certain situations. The algorithm was developed and adjusted to achieve the major applicability by implementing a typical fix for general faults in all images. The algorithm was subsequently applied to eight datasets of cotton with different growth stages to target the general problems for all images. In total, the algorithm was applied to 252 images of cotton plants and 20 images of hibiscus plants. Three illumination conditions were considered to examine the algorithm's reliability under a variety of situations. Table 2 labels these conditions as: 'sunny' for clear sky, 'shady' for sun with shade, and 'cloudy' for complete cloud cover. Table 2 also shows the solar energy values on these days for the cotton plant datasets. To evaluate its reliability, the developed algorithm was applied to plants other than cotton (hibiscus). The hibiscus plant images were captured during Autumn 2013 under the same conditions of cotton plants. The results were subdivided according to plant size, big cotton and small cotton, for each dataset. The performance of the developed algorithm was evaluated using the following metrics:

1. True Positive (TP): Refers to a true plant leaf correctly identified by the developed algorithm.
2. False Negative (FN): Represents a plant leaf incorrectly identified as a non-leaf.
3. False Positive (FP): Represents a non-leaf incorrectly identified as a true plant leaf, or a large and bent leaf identified twice.
4. True Negative (TN): Refers to a non-leaf correctly identified as a non-leaf. This metric was not considered during the accuracy calculation, owing to the uncountable number of objects in the image that are truly identified as non-leaf objects.

For each dataset, the sensitivity (recall), precision, accuracy and F-measure were calculated using Eqs. (4.1)-(4.4), respectively [50,73,74]:

$$Sensitivity = \frac{TP}{TP + FN} \times 100\% \quad (4.1)$$

$$Precision = \frac{TP}{TP + FP} \times 100\% \quad (4.2)$$

$$Accuracy = \frac{TP + TN}{TP + FN + TN + FP} \times 100\% \quad (4.3)$$

$$F - measure = \frac{2TP}{2TP + FP + FN} \times 100\% \quad (4.4)$$

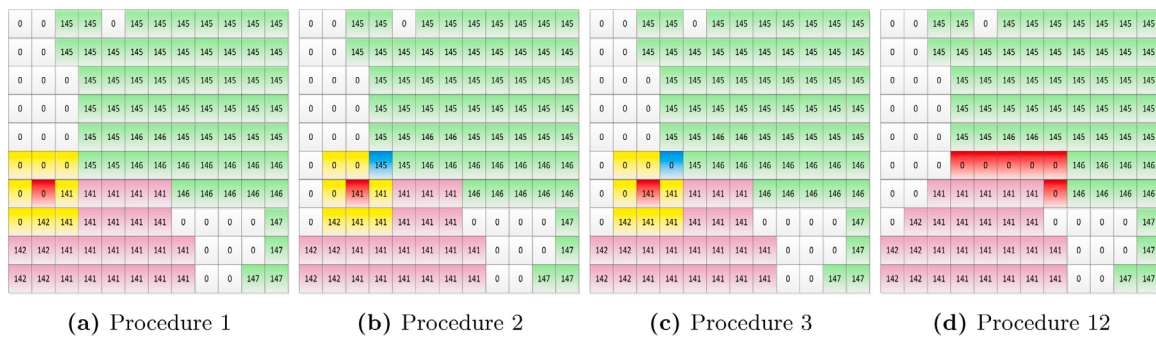


Fig. 11. Leaves segmented using (ENBD) technique; the red pixel presents the centre of the window, the yellow pixels present the eight neighbouring pixels, and the blue pixel presents the changed pixel after the application of this technique. (For interpretation of the references to colour in this figure legend, the reader is referred to the web version of this article.)

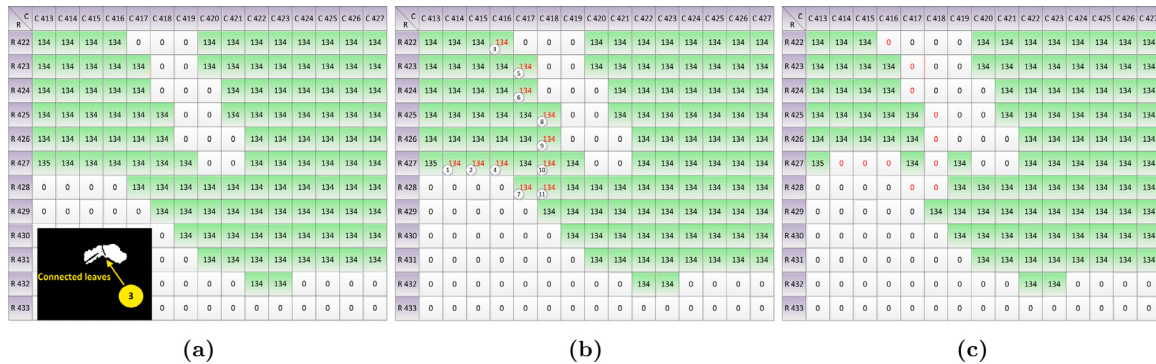


Fig. 12. Disparity map of area 3 connected leaves: (a) Two areas of plant 3 connected by a small number of pixels and the disparity map of the same connected area. (b) Sequence of the ZNC technique. (c) Disparity map after the separation of the two connected areas using the ZNC technique.

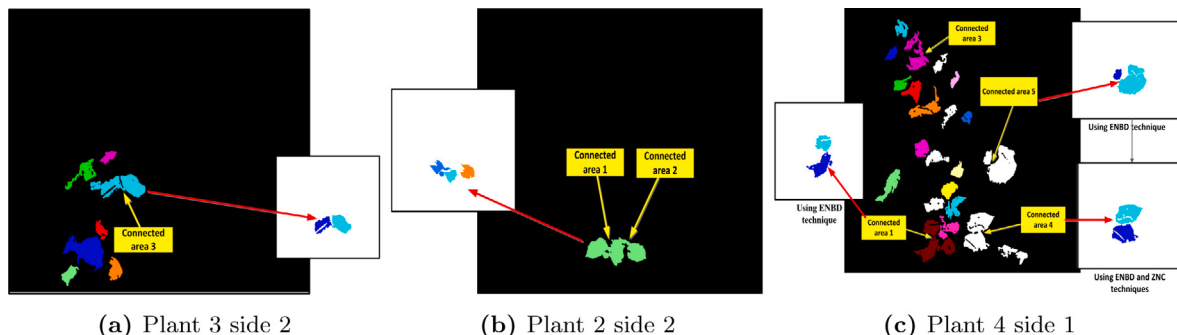


Fig. 13. (a) Colour image of area 3, plant 3 after separation using ENBD and ZNC techniques, (b) Plant 2 final segmentation image after using DDS techniques, (c) Different areas of plant 4 after separation using ENBD and ZNC techniques. (For interpretation of the references to colour in this figure legend, the reader is referred to the web version of this article.)

Table 1
Final leaf segmentation results for the 8 selected cotton and hibiscus plants in Figs. Fig. 14.

Name of technique	Total leaf auto-count	Total leaf visual image count	False negative	False positive	Total true segments	Accuracy%
Image pre-processing	95	122	4	31	91	72
DMD	98	122	4	28	94	75
GDS	106	122	4	20	102	81
ENBD	112	122	5	15	107	84
ENBD+ZNC	120	122	5	7	115	91

4.1. Results evaluation

The main challenge for the proposed algorithm was the segmentation of complex-structured plant leaves with many occlusion boundaries under variable outdoor conditions. Although outdoor images have

many challenges and difficulties issues such as partial shadow and overexposed areas emerged as result of the illumination in outdoor conditions. Plant leaves were efficiently segmented from the natural background according to their colour, shape, and depth properties.

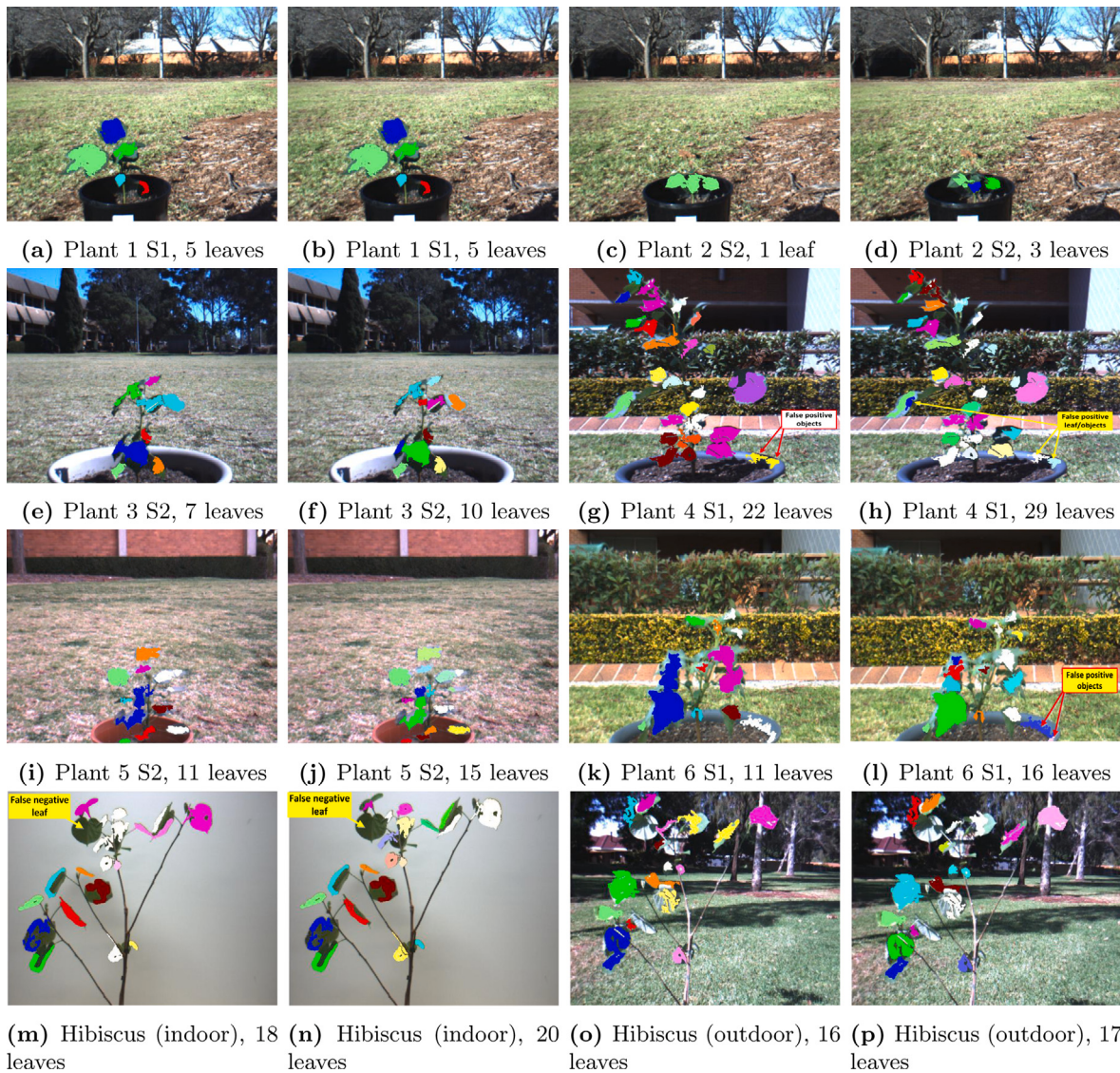


Fig. 14. Final leaf segmentations for the eight plants of Fig. 1. Columns 1 and 3 present results after using the image pre-processing algorithm; columns 2 and 4 show results after using DDS algorithm.

Table 2

Cotton plants data set collection. The images were collected during Winter and early Spring of 2014.

Data sets	Image condition	Sun direction	Solar energy (Watts/m ²)
Dataset 1 (July 13, 12–4 pm)	Sunny	Multiple	178–640
	Some overexposed and partial shading of leaves	From left, right and behind the camera	
Dataset 2 (July 14, 10 am–2 pm)	Shady	N/A	N/A
	Low illumination		
Dataset 3 (August 8, 12–4 pm)	Sunny	Single	273–714
	Overexposed leaves	From right side of the camera only	
Dataset 4 (August 9, 11 am–2 pm)	Shady	N/A	N/A
	Low illumination		
Dataset 5 (August 28, 1–4 pm)	Sunny	Single	285–780
	Wind and some bluer image	From behind the camera only	
Dataset 6 (August 26, 12–3 pm)	Cloudy	N/A	77–183
	Complete cloud cover		
Dataset 7 (September 19, 11 am–3 pm)	Sunny	Single	253–892
	Some overexposed and partial shading of leaves	From left side of the camera only	
Dataset 8 (September 19, 3–6 pm)	Shady	N/A	N/A
	Low illumination		

The accuracy of the proposed algorithm was evaluated by the comparison between the number of leaves produced from automatic segmentation, and the number obtained from visual counting from plant images. The tested datasets had 272 image pairs (colour image

and disparity map) with 2453 cotton and hibiscus leaves in total. The use of the developed segmentation algorithm was able to successfully detect 1910 leaves with a segmentation rate of 78% for individual plant leaves. The separation of occluded leaves was carried out using the

Table 3

Total segmentation rates of developed algorithm for cotton and hibiscus plants under all conditions where, A = Accuracy, S = Sensitivity, P = Precision and F = F-measure.

Condition	All environmental & lighting conditions				
	No. of images	A%	S%	P%	F%
Big cotton	64	70	80	86	83
Small cotton	188	69	76	89	82
Hibiscus	20	73	78	92	85
Overall rates	272	71	78	89	83

proposed DDS algorithm. A high separation rate of 84% was observed, where 484 leaves could be separated successfully from 578 connected and overlapped leaves.

Table 3 below shows the overall detection rates of cotton and hibiscus plants under different illumination conditions. The table also shows approximately the same performance for both plants with no significant difference observed between the results for small and big cotton plants. **Fig. 14** shows some examples of plant images with many leaves in various positions and shapes (single, touching, and overlapping) that were detected successfully.

The segmentation accuracy, sensitivity, precision and F-measure for hibiscus plants were slightly higher than for cotton (**Table 3**). The higher results were expected owing to the difference in structure between cotton and hibiscus plants and the location of where the images were taken (indoor). **Table 4** illustrates acceptable segmentation rates of cotton leaves for shady and cloudy conditions compared to sunny conditions. This is due to the images being overexposed by sun conditions or affected by partial shadow issues. Nevertheless, the shady conditions can have low illumination or insufficient light coverage, resulting in false negative and false positive leaves for some images taken in the shade.

Small cotton plants reveal very similar accuracy rates (68%) for both sunny and shady conditions, but a higher accuracy rate for cloudy conditions (73%) has been reported. Overall, the segmentation rate of both cotton sizes was adequate; however, the images were affected by outdoor environment issues such as direct sunlight and distant trees. Similarly, the diversity of conditions for hibiscus plant images produced different segmentation rates. As the hibiscus plant was not the main focus of this study, the sample size of hibiscus plant images was not as large as that of cotton images. High rates of accuracy were observed for hibiscus plants under indoor (80%) and shady (79%) conditions, whereas medium rates of accuracy were achieved for sunny (67%) and cloudy (65%) conditions.

4.2. Results discussion

The algorithm was evaluated under sunny, shady, and cloudy conditions. A certain test was conducted to examine one illumination condition for each dataset revealed different illuminations issues. In addition, other images present the effects of other leaf factors such as touching and overlapping leaves, leaf orientation and leaf size. The following subsections will analyse the impact of these factors on the segmentation results. The results show that certain images from different datasets had insufficient light coverage, such as partial shadow or low-light conditions, whereas other images exhibited overexposed areas.

4.2.1. Partial shadow

The shaded leaf could possibly be recognised as two leaves or one leaf that has inadequate information for a positive leaf identification using depth properties. This is owing to a leaf with two different areas (shaded, unshaded) potentially producing incorrect depth information since the correlation between the stereo pair of images depends on the brightness pixels of the edge image rather than the absolute values.

Table 4

Average segmentation rates for cotton plants under different illumination conditions where, A = Accuracy, S = Sensitivity, P = Precision and F = F-measure.

Pot size	Big cotton						Small cotton				
	Lighting	No. of image	A%	S%	P%	F%	No. of image	A%	S%	P%	F%
Sunny		32	69	76	87	81	94	67	73	91	81
Shady		24	71	84	84	84	70	68	79	85	82
Cloudy		08	71	83	83	83	24	73	80	90	85

Furthermore, the shady areas could appear as dark areas in the images (that could include various plant parts). These dark areas can affect the HSV colour transformation of the hue channel, whereas it is hard to differentiate between a leaf and non-leaf object according to its colour. The depth information was also considered for these shaded regions because they are within the threshold value of depth that segments the plant from the background. Therefore, the image analysis algorithm may count shaded regions as a real leaf, causing false positive leaf issues.

For some images, shadows were cast behind the plant when sunlight came from the back of the camera facing the plant. This case was considered an outstanding example of capturing images under sunny conditions. Nevertheless, images were captured from different directions (left, right) with respect to the camera as plants can experience sunlight from different directions during the day. For some instances, leaves under shadow are also segmented correctly by the algorithm. The reason behind this is the colours of these leaves are still within the green area of the hue channel, despite the difference in illumination as discussed in Section 3.1.2. The front sunlight direction caused camera overexposure; therefore, the image analysis of front sun direction was not considered or evaluated due to the camera overexposure issue. **Fig. 15** shows three plants with different sun directions.

4.2.2. Low illumination

The low-illumination conditions were observed in two cases: during sunset; and in shady area, where it is difficult to recognise all the leaves from the visual inspection of the colour images. The shady condition occurred when the plant was placed in the shade, while the camera was set between the plant (facing the plant) and the shady source. **Fig. 16** presents an image of the plant taken under shadow in the morning (**Fig. 16a**), but a high segmentation rate is observed. In contrast, another plant image was taken under the same condition but show low segmentation rates (**Fig. 16c**). The analysis of the colour images and disparity maps shows that most of the plants' leaves were produced by the stereo vision system (**Fig. 16b**), whereas many of the plant's leaves are missing from the disparity maps of **Fig. 16d**. This contradictory is due another factor, leaf orientation (i.e. the direction of a leaf with respect to the camera). **Fig. 16c** shows back or obscured directions for the majority of the plants' leaves, whereas images of **Fig. 16a** present leaves with front-dominant directions. A front-dominant leaf direction can offer the required leaf texture for calculating accurate and dense depth values and preserve a complete leaf shape. In contrast, the depth values might compute for a few points for the low-textured object [75].

4.2.3. Overexposure

Overexposure was observed in most of the sunny condition images owing to the reflected sunlight by the overexposed areas towards the camera sensors. These images may not be segmented correctly, hence these images exhibited the issue of false negative leaves. Leaves which are overexposed are yellow rather than green. This lighting issue was investigated for the plant in **Fig. 17a**. The disparity map and the RGB colour transformation (Section 3.1.1) present these overexposed leaves, as shown in **Figs. 17b** and **17c**, respectively. The histogram distribution shows that the maximum number of bins are within the yellow area of the hue channel (**Fig. 17d**), while other histogram bins lie between the green and red areas.

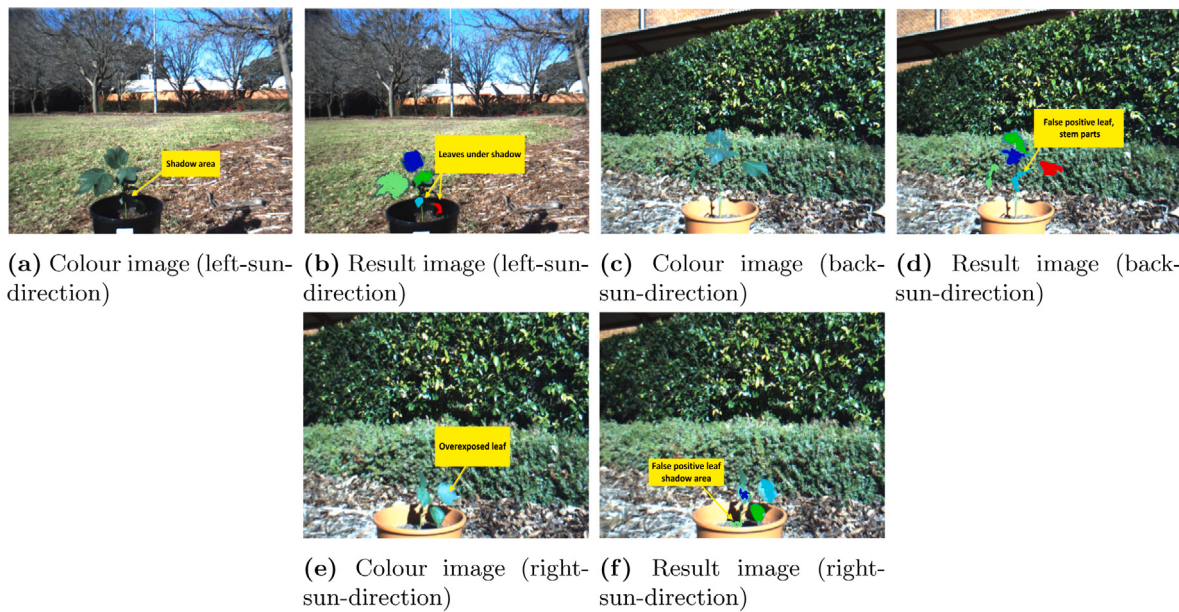


Fig. 15. Three selected plants from dataset 1 with different sun directions.

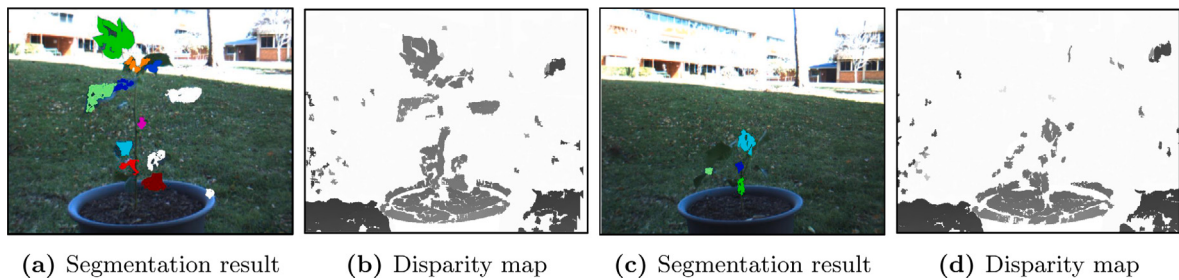


Fig. 16. Tow selected plants from different datasets with low-lighting condition (shady areas). (a) and (b) show high segmentation rates. (c) and (d) show low segmentation rates. (For interpretation of the references to colour in this figure legend, the reader is referred to the web version of this article.)

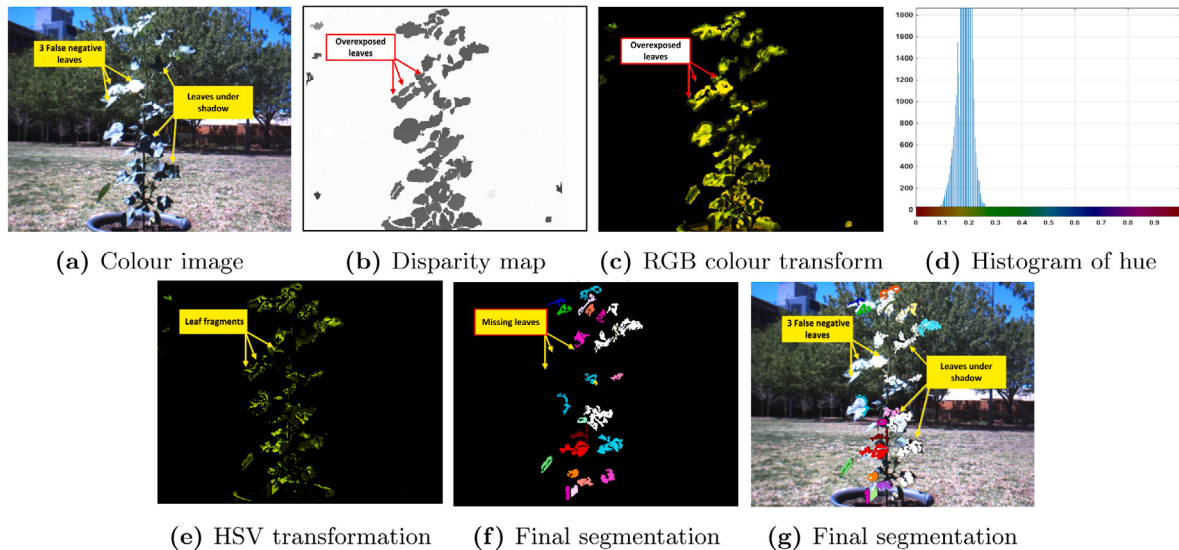


Fig. 17. Steps of segmentation for plant 3 side 2 from dataset 5 (big cotton) with overexposed and partial shadow conditions. (For interpretation of the references to colour in this figure legend, the reader is referred to the web version of this article.)

Since the adopted techniques filter out the hue channel for green only and eliminates the yellow areas as discussed in Section 3.1.2. Therefore, these leaves appear as small fragments of green areas

(Fig. 17e) which are removed when applying image enhancement processes (Section 3.1.3), as shown in Figs. 17f and 17g. Addressing this issue by changing the calibration parameters of Eqs. (3.1) and (3.2)

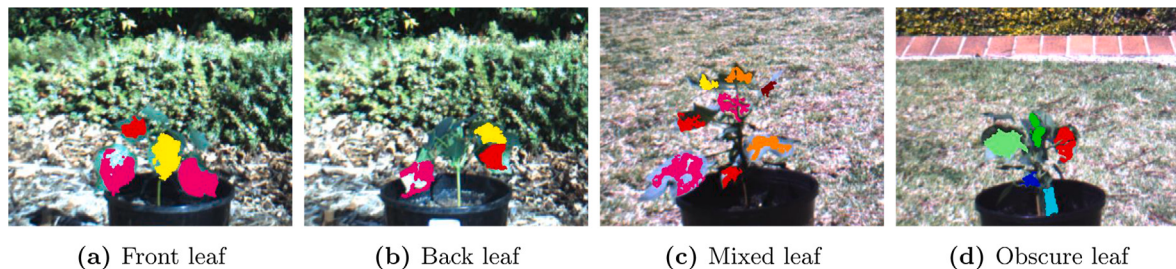


Fig. 18. Four selected plants with different dominant leaf orientations.

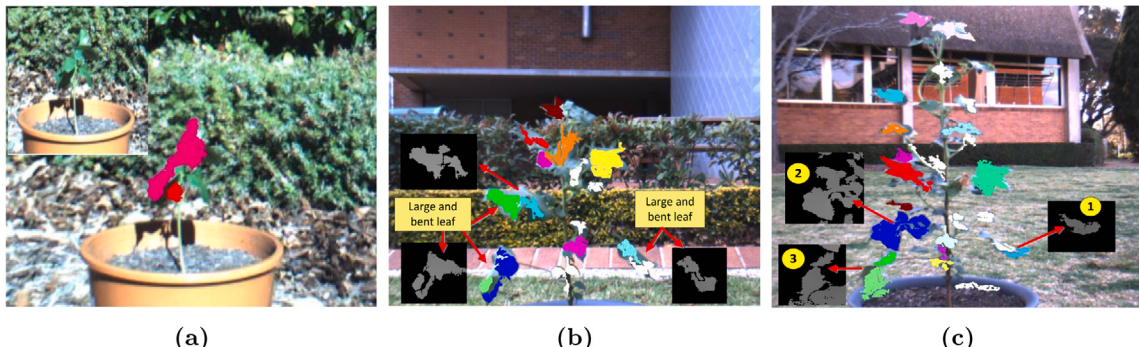


Fig. 19. Plants with different leaf sizes: (a) Small cotton with four small leaves incorrectly segmented as one leaf; (b) big cotton with three large and bent leaves showing two-part disparity for each leaf; and (c) big cotton with three large and bent leaves showing one-part disparity for each leaf.

to accept yellow-hue pixels as well as green pixels caused another issue, whereby non-leaf objects could also be identified as true leaves. Overexposure is a challenging issue for machine vision under outdoor conditions, which invites further studies and analysis to solve this critical problem. The analysis of the effect of lighting on the segmentation result strongly supports the argument for the reliability of the stereo vision system under different outdoor illumination conditions. The analysis also supports and illustrates the limitation of this system to work with a low-textured scene. To overcome the feature mismatching issue under unstable illumination condition at outdoors, one of the future solutions is to use the Terrestrial laser scanners (TLS), based laser scanning (LiDAR). This sensor was successfully used by [76–78] to quantify plant features and to reconstruct a 3D model of a plant. It produces a high density scan necessary for capturing small objects such as leaves and has longer range than the 2.5 sensors which is more suitable for field applications.

4.2.4. Effect of leaf orientation

Leaf orientation is an important factor to provide sufficient leaf texture for an accurate stereo matching process. The impact of this factor on the performance of the algorithm was investigated. During data collection, the front side of the plant was labelled as side 1, where all of the leaves' upper surfaces faced the camera. Consequently, the back side of the plant was labelled as side 2, where all of the leaves' lower surfaces faced the camera. Typically, these two ideal cases were observed for some plants. For the majority of the images, the view was mixed between front, side, and back leaves. The leaf segmentation rates with respect to the leaf orientation for all cotton plants are presented in Table 5. Fig. 18 shows four selected plants with different types of leaf orientation. A higher segmentation rate was observed for the front-dominant leaf orientation compared with the orientation of other leaves. This is due to the complete leaf shape with full texture information showing by this orientation (Fig. 18a). Owing to insufficient colour, texture, shape, and depth information being detected, it is difficult to detect back dominant leaf orientation, as shown in Fig. 18b. Mixed dominant leaf images show adequate segmentation rates (Fig. 18c). However, some leaves appeared as a thin

Table 5
All data sets segmentation results according to leaf orientation.

Plant size	Big and small cotton				
	Leaf orientation	No. of image	Accuracy%	Sensitivity%	Precision%
Front dominant	35	79	86	91	85
Back dominant	11	70	77	89	83
Mix dominant	166	69	77	88	82
Obscure-leaf-orientation	40	65	73	85	79

line (similar to a stem and branches), which potentially insinuates that there is insufficient information for a positive leaf identification and could not be identified correctly as a leaf when applying ellipse criteria (Section 3.1.3). Leaf movement due to the wind or the small leaf size at an early growth stage of the plant can cause an obscure leaf shape and a blurred image which is difficult to recognise and segment (Fig. 18d).

4.2.5. Effect of leaf size

Different leaf sizes could be observed in one plant image, ranging from 1 to 10 cm as a plant grows. Fig. 19a shows a plant with four small leaves, which are incorrectly segmented as two leaves due to the difficulty associated with distinguishing between them using visual inspection. Large and bending leaves (larger than 10 cm) were significantly noticeable in big cotton plant images as shown in Figs. 19b and 19c. These leaves exhibit bending around each lobe, causing distinct depth differences (greater than three pixels in the disparity map) for different lobes of a single leaf. Fig. 19c shows the colour image and the corresponding disparity maps where some leaves are agglomerated in one part with a flat pose and different lobes. These leaves could be segmented adequately by the algorithm and identified precisely as one leaf as shown by leaf 2. In contrast, large and bent leaves are a critical segmentation issue, as they are normally divided into two parts owing to the distinct difference in depth as shown in Fig. 19b. Each part of these leaves was segmented and considered as an independent leaf by the DDS algorithm as shown by leaf 1 and leaf 3 in Fig. 19c. From 252 cotton images, approximately 67 leaves were visually assigned as

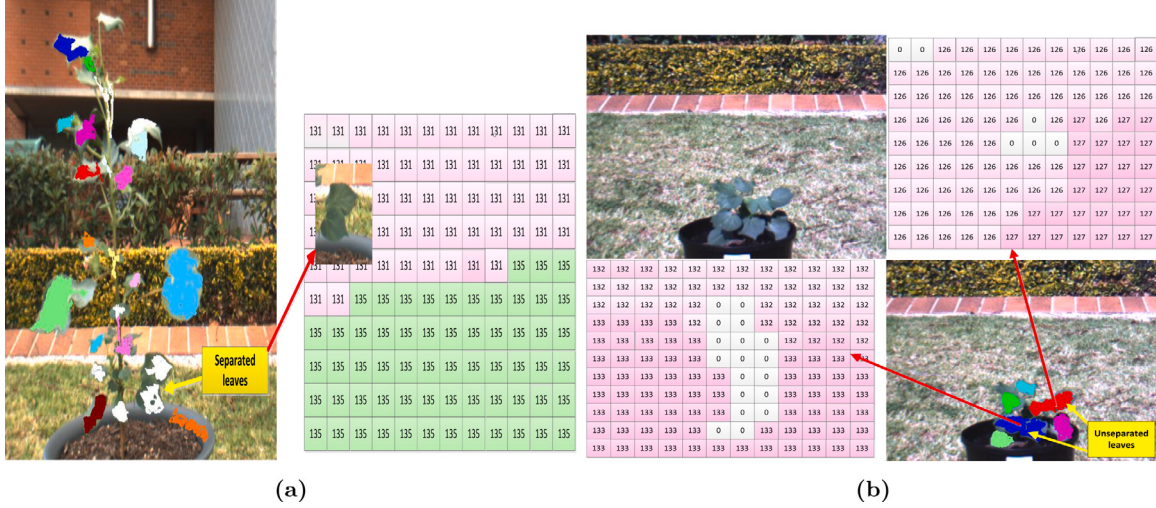


Fig. 20. Two selected plants with overlapping leaves in flat pose and their segmentation results: (a) Unseparated leaves; (b) separated leaves.

large, bent, and folded leaves. These leaves produced 26 objects as false positive leaves, which is 10% of the total number of false positive leaves.

4.2.6. Effect of overlapped leaves

The connected and overlapped leaves with flat poses are a critical segmentation issue for the developed algorithm. Fig. 20a shows a big cotton plant with two overlapping leaves with a flat pose and the corresponding disparity map. These leaves were correctly segmented into two leaves using the depth property (more than three pixels difference). In contrast, Fig. 20b presents a small cotton plant with four connected leaves and their corresponding disparity maps for each connected pair. These connected leaf areas were incorrectly identified as a single leaf for each pair because the difference between the neighbouring pixels is less than the threshold value. In this instance, the depth feature would not be beneficial to segment this particular type of occluded leaf. Therefore, the algorithm would need to extract other features such as leaf boundary shape attributes from the images using different techniques. Table 6 shows the total number of connected and overlapped leaves for cotton and hibiscus plants with their segmentation rates.

4.2.7. Comparison with previous work

A brief comparison between the performance of several previous research work and our proposed work in term of segmenting individual leaves and separating the overlapping leaves is presented. There are several differences among the used methods including the sensor used, the viewpoint (2D, 2.5D or 3D) or the environmental conditions (indoor, green house, outdoor) which affect segmentation rates. The percentage (%) metric of the successful segmentation rates was used to compare segmentation methods. Most of these methods concern non-occluded leaves segmentation. The following comparison only includes methods that conducted leaf segmentation and overlapping leaves separation. Table 7 illustrates a summary of these methods.

[1] developed multiple leaf segmentation method based on prior knowledge of leaf shapes using 2D sensor. The method utilised quadratic Bezier curve fitting and Multilayer Perceptron Classifier (MLP). A modified Active Shape Model technique was applied to implement the matching and identification process to identify single, connected, and overlapped leaves under greenhouse illumination conditions. Although good segmentation rates were presented by the method, it has limitations for applying this method to other plants which exhibit different leaf shapes in addition to its computation time cost.

[44] used mean shift algorithm on the colour space to remove background. Then, an active contour model was applied on the depth

data to segment plant leaves and targeted the overlapped leaves under controlled illumination conditions. [47] proposed a method for reconstructing point cloud from two stereo image. The method was focused on stereo matching algorithm more than leaf segmentation. Image experiment was conducted with a few images of one plant under different illumination conditions. Later they address the overlapping issue in [50] by developing a new 3D joint filter operator method. Their method used three different techniques to reconstruct the 3D model of the plant and achieved high segmentation rates, however, there are some limitations related to complexity of shape based detection method and cannot work under direct sun light conditions. [55] utilised 2D colour sensor and SfM method to reconstruct a 3D model of plant. Leaves in the 3D model were segmented based on top view images using distance transform and watershed algorithm. The segmented seed regions are then projected on the voxel 3D model. Next, the attribute-expanding method was employed to expand the seed voxel regions until all voxel neighbours were fully assigned and the missing parts of the occluded leaves were completed.

The comparison between different leaf segmentation methods should be taken with caution due to the significant different in sensors used, size of dataset, type of plants as well as the environment conditions. A close look on Table 7 and the segmentation results shows, the use of the 2D sensor [1] revealed lower rate in segmenting individual and overlapped leaves of four types of plants under greenhouse environments. Contrary to that, the use of depth data from 2.5D sensor as in [44,47,50] and 3D model of plants as [50,55] improved the rate of segmentation. The results presented by our work add advantages where a good segmentation rate was achieved by using a single viewpoint of disparity maps. Most of these results were achieved for images taken under different outdoor illumination conditions (direct sunlight) which open a new future work prospect.

5. Conclusion

This paper demonstrates the development of a new image analysis algorithm to segment overlapping leaf boundaries. An effort was made to find the best method of consistently segmenting leaves from different aspects of plant images. The images were acquired by a stereo vision sensor in semi-structured outdoor environments under a variety of sunlight conditions (sunny, shady, and cloudy). The developed method (DDS) depends on the depth feature without adding any artificial tags on the leaves. This method is based on searching for discontinuities in depth using global and local methods. The algorithm was evaluated through a variety of experimental tests with two differently

Table 6

Separation rate of DDS algorithm for occluded and overlapping leaves for cotton and hibiscus plants in all conditions.

Condition	All environmental & lighting conditions					
Plant type	No. of image	No. of leaf	Segmented leaf	Overlapped leaves	Separated	Separation rate%
Cotton	252	2025	1578	514	431	84%
Hibiscus	20	428	323	64	53	83%
Overall rates	272	2453	1910	578	484	84%

Table 7

Comparison of percentage of successful segmentation rates.

Study	Sensors	Viewpoint	Environments	Segmented leaf	Segmentation rates %
[1]	Colour camera	2D	Greenhouse	217 individual 524 overlapping	47.1–85.7% 21.6–87.8%
[44]	Kinect v1	2.5D	Greenhouse	114 individual 360 overlapping	92.10% 86.67%
[47]	Stereo camera	2.5D	Indoors Greenhouse Outdoors	37	94.59%
[50]	Kinect v2 Stereo camera Colour image	2.5D 2.5D 3D	Indoors Greenhouse Outdoors	102 76	99.33%
[55]	Colour camera	3D	Indoors	61	75%–100%
Ours	Stereo camera	2.5D	Outdoors (Sunny Cloudy Shady) Indoors	1910 individual 484 overlapping	78% 84%

structured plants, cotton, and hibiscus. An enhancement in leaf detection was observed when utilising a combination of image features rather than using each feature separately. The algorithm successfully detected individual plants' leaves and segmented the small clusters of the overlapping leaves with detection and separation rates of 78% and 84%, respectively. The results show almost identical performance for both plants under various conditions. This method is potentially applicable to other types of plants with similar structures to cotton and hibiscus. Overexposure, leaf orientation, and the occlusion between leaf boundaries are the main issues that affected the segmentation accuracy. Future work will focus on exploring the ability of using machine learning techniques specifically Convolutional Neural Networks (CNNs) algorithm to implement the fusion of colour and depth data to effectively isolate leaf pixels from background and other parts of plant.

CRediT authorship contribution statement

Zainab Mohammed Amean: Conceptualization, Methodology, Software, Data curation, Validation, Writing. **Tobias Low:** Supervision. **Nigel Hancock:** Supervision.

Declaration of competing interest

The authors declare that they have no known competing financial interests or personal relationships that could have appeared to influence the work reported in this paper.

Acknowledgments

This work was supported by the University of Southern Queensland, Toowoomba, Australia. The first author would like to acknowledge the Iraqi Ministry of Higher Education and the University of Technology, Iraq for funding the PhD scholarship.

References

- [1] Xia C, Lee J-M, Li Y, Song Y-H, Chung B-K, Chon T-S. Plant leaf detection using modified active shape models. Biosyst Eng 2013;116(1):23–35.
- [2] De Mezzo B, Rabatel G, Fiorio C. Weed leaf recognition in complex natural scenes by model-guided edge pairing. In: Precision agriculture. 2003, p. 141–7.
- [3] Slaughter D, Giles D, Downey D. Autonomous robotic weed control systems: A review. Comput Electron Agric 2008;61(1):63–78.
- [4] Feng PC, Brinker RJ. Methods for weed control using plants having dicamba-degrading enzymatic activity. 2010, US Patent 7, 855, 326.
- [5] Gongal A, Silwal A, Amatya S, Karkee M, Zhang Q, Lewis K. Apple crop-load estimation with over-the-row machine vision system. Comput Electron Agric 2016;120:26–35.
- [6] Zhou Z, Morel J, Parsons D, Kucheryavskiy SV, Gustavsson A-M. Estimation of yield and quality of legume and grass mixtures using partial least squares and support vector machine analysis of spectral data. Comput Electron Agric 2019;162:246–53.
- [7] Koirala A, Walsh KB, Wang Z, McCarthy C. Deep learning—method overview and review of use for fruit detection and yield estimation. Comput Electron Agric 2019;162:219–34.
- [8] Chaudhary P, Chaudhari AK, Cheeran A, Godara S. Color transform based approach for disease spot detection on plant leaf. Int J Comput Sci Telecommun 2012;3(6):65–70.
- [9] Arivazhagan S, Shebiah RN, Ananthi S, Varthini SV. Detection of unhealthy region of plant leaves and classification of plant leaf diseases using texture features. Agric Eng Int: CIGR J 2013;15(1):211–7.
- [10] Wspanialy P, Moussa M. Early powdery mildew detection system for application in greenhouse automation. Comput Electron Agric 2016;127:487–94.
- [11] Singh V, Misra AK. Detection of plant leaf diseases using image segmentation and soft computing techniques. Inf Process Agric 2017;4(1):41–9.
- [12] Singh V. Sunflower leaf diseases detection using image segmentation based on particle swarm optimization. Artif Intell Agric 2019;3:62–8.
- [13] Tian K, Li J, Zeng J, Evans A, Zhang L. Segmentation of tomato leaf images based on adaptive clustering number of k-means algorithm. Comput Electron Agric 2019;165:104962.
- [14] Raina S, Gupta A. A study on various techniques for plant leaf disease detection using leaf image. In: 2021 international conference on artificial intelligence and smart systems (ICAIS). IEEE; 2021, p. 900–5.
- [15] Saputra TW, Masithoh RE, Achmad B. Development of plant growth monitoring system using image processing techniques based on multiple images. In: Proceeding of the 1st international conference on tropical agriculture. Springer; 2017, p. 647–53.
- [16] Trivedi M, Gupta A, et al. Automatic monitoring of the growth of plants using deep learning-based leaf segmentation. Int J Appl Sci Eng 2021;18(2):1–9.
- [17] Yanikoglu B, Aptoula E, Tirkaz C. Automatic plant identification from photographs. Mach Vis Appl 2014;25(6):1369–83.

- [18] Chien C, Lin T. Leaf area measurement of selected vegetable seedlings using elliptical hough transform. *Trans ASAE* 2002;45(5):1669–77.
- [19] Franz E, Gebhardt M, Unklesbay K. Shape description of completely visible and partially occluded leaves for identifying plants in digital images. *Trans ASAE* 1991;34(2):673–0681.
- [20] Franz E, Gebhardt M, Unklesbay K. Algorithms for extracting leaf boundary information from digital images of plant foliage. *Trans ASAE* 1995;38(2):625–33.
- [21] Chien C, Lin T. Non-destructive growth measurement of selected vegetable seedlings using orthogonal images. *Trans ASAE* 2005;48(5):1953–61.
- [22] Dellen B, Scharr H, Torras C. Growth signatures of rosette plants from time-lapse video. *IEEE/ACM Trans Comput Biol Bioinform* 2015;12(6):1470–8.
- [23] Kumar JP, Domnic S. Image based leaf segmentation and counting in rosette plants. *Inf Process Agric* 2019;6(2):233–46.
- [24] Gupta A, Prakash D. A fast and efficient color model for automatic monitoring of plants based on leaf images. *Computing* 2020;7(17):2020.
- [25] Neto JC, Meyer GE, Jones DD. Individual leaf extractions from young canopy images using gustafson-kessel clustering and a genetic algorithm. *Comput Electron Agric* 2006;51(1):66–85.
- [26] Pan J, He Y. Recognition of plants by leaves digital image and neural network. In: Computer science and software engineering, 2008 international conference on, Vol. 4. IEEE; 2008, p. 906–10.
- [27] Ozturk S, Akdemir B. Automatic leaf segmentation using grey wolf optimizer based neural network. In: 2017 electronics. IEEE; 2017, p. 1–6.
- [28] Lee W, Slaughter D. Recognition of partially occluded plant leaves using a modified watershed algorithm. *Trans ASAE* 2004;47(4):1269.
- [29] Wang X-F, Huang D-S, Du J-X, Xu H, Heutte L. Classification of plant leaf images with complicated background. *Appl Math Comput* 2008;205(2):916–26.
- [30] Tang X, Liu M, Zhao H, Tao W. Leaf extraction from complicated background. In: Image and signal processing, 2009. CISP'09. 2nd international congress on. IEEE; 2009, p. 1–5.
- [31] Nesaratnam J, BalaMurugan C. Identifying leaf in a natural image using morphological characters. In: Innovations in information, embedded and communication systems (ICIIECS), 2015 international conference on. IEEE; 2015, p. 1–5.
- [32] Viaud G, Loudet O, Courrière P-H. Leaf segmentation and tracking in arabidopsis thaliana combined to an organ-scale plant model for genotypic differentiation. *Front Plant Sci* 2017;7:2057.
- [33] De Vylder J, Ochoa D, Philips W, Chaerle L, Van Der Straeten D. Leaf segmentation and tracking using probabilistic parametric active contours. In: International conference on computer vision/computer techniques and applications. Springer; 2011, p. 75–85.
- [34] Yin X, Liu X, Chen J, Kramer DM. Joint multi-leaf segmentation, alignment, and tracking for fluorescence plant videos. *IEEE Trans Pattern Anal Mach Intell* 2017;40(6):1411–23.
- [35] Yu J-G, Li Y, Gao C, Gao H, Xia G-S, Yu ZL, Li Y. Exemplar-based recursive instance segmentation with application to plant image analysis. *IEEE Trans Image Process* 2019;29:389–404.
- [36] Pape J-M, Klukas C. 3-d histogram-based segmentation and leaf detection for rosette plants. In: European conference on computer vision. Springer; 2014, p. 61–74.
- [37] Xu L, Li Y, Sun Y, Song L, Jin S. Leaf instance segmentation and counting based on deep object detection and segmentation networks. In: 2018 joint 10th international conference on soft computing and intelligent systems (SCIS) and 19th international symposium on advanced intelligent systems (ISIS). IEEE; 2018, p. 180–5.
- [38] Chapron M, Ivanov N, Boissard P, Valery P. Visualization of corn acquired from stereovision. In: Systems, man and cybernetics, 1993.'systems engineering in the service of humans', conference proceedings. International conference on. Vol. 5. IEEE; 1993, p. 334–8.
- [39] Andersen HJ, Reng L, Kirk K. Geometric plant properties by relaxed stereo vision using simulated annealing. *Comput Electron Agric* 2005;49(2):219–32.
- [40] Takizawa H, Ezaki N, Mizuno S, Yamamoto S. Measurement of plants by stereo vision for agricultural applications. In: Signal and image processing: Proceedings of the seventh IASTED international conference. 2005.
- [41] Mizuno S, Noda K, Ezaki N, Takizawa H, Yamamoto S, Graphics Collaboration. Detection of will by analyzing color and stereo vision data of plant. *Comput Vis/Comput Tech* 2007;400–11.
- [42] Wallenberg M, Felsberg M, Forssén P-E, Dellen B. Channel coding for joint colour and depth segmentation. In: Joint pattern recognition symposium. Springer; 2011, p. 306–15.
- [43] Chéné Y, Rousseau D, Lucidarme P, Bertheloot J, Caffier V, Morel P, Belin É, Chapeau-Blondeau F. On the use of depth camera for 3d phenotyping of entire plants. *Comput Electron Agric* 2012;82:122–7.
- [44] Xia C, Wang L, Chung B-K, Lee J-M. In situ 3d segmentation of individual plant leaves using a rgb-d camera for agricultural automation. *Sensors* 2015;15(8):20463–79.
- [45] Zhang Y, Teng P, Shimizu Y, Hosoi F, Omasa K. Estimating 3d leaf and stem shape of nursery paprika plants by a novel multi-camera photography system. *Sensors* 2016;16(6):874.
- [46] Xiong X, Yu L, Wang Y, Liu M, Jiang N, Wu D, Chen G, Xiong L, Liu K, Liu Q. A high-throughput stereo-imaging system for quantifying rape leaf traits during the seedling stage. *Plant Methods* 2017;13(1):1–17.
- [47] Li D, Xu L, Tang X-s, Sun S, Cai X, Zhang P. 3d imaging of greenhouse plants with an inexpensive binocular stereo vision system. *Remote Sens* 2017;9(5):508.
- [48] Milella A, Marani R, Petitti A, Reina G. In-field high throughput grapevine phenotyping with a consumer-grade depth camera. *Comput Electron Agric* 2019;156:293–306.
- [49] Li D, Cao Y, Tang X-s, Yan S, Cai X. Leaf segmentation on dense plant point clouds with facet region growing. *Sensors* 2018a;18(11):3625.
- [50] Li D, Cao Y, Shi G, Cai X, Chen Y, Wang S, Yan S. An overlapping-free leaf segmentation method for plant point clouds. *IEEE Access* 2019;7:129054–70.
- [51] Alenyà G, Dellen B, Foix S, Torras C. Robotized plant probing: Leaf segmentation utilizing time-of-flight data. *IEEE Robot Autom Mag* 2013;20(3):50–9.
- [52] Yau WK, Ng O-E, Lee SW. Portable device for contactless, non-destructive and in situ outdoor individual leaf area measurement. *Comput Electron Agric* 2021;187:106278.
- [53] Kazmi W, Foix S, Alenyà G, Andersen HJ. Indoor and outdoor depth imaging of leaves with time-of-flight and stereo vision sensors: Analysis and comparison. *ISPRS J Photogramm Remote Sens* 2014;88:128–46.
- [54] Liu X, Hu C, Li P. Automatic segmentation of overlapped poplar seedling leaves combining mask r-cnn and dbscan. *Comput Electron Agric* 2020;178:105753.
- [55] Itakura K, Hosoi F. Automatic leaf segmentation for estimating leaf area and leaf inclination angle in 3d plant images. *Sensors* 2018;18(10):3576.
- [56] Itakura K, Hosoi F. Automatic method for segmenting leaves by combining 2d and 3d image-processing techniques. *Appl Opt* 2020;59(2):545–51.
- [57] Golbach F, Kootstra G, Damjanovic S, Otten G, van de Zedde R. Validation of plant part measurements using a 3d reconstruction method suitable for high-throughput seedling phenotyping. *Mach Vis Appl* 2016;27(5):663–80.
- [58] Mozos OM, Mizutani H, Kurazume R, Hasegawa T. Categorization of indoor places using the kinect sensor. *Sensors* 2012;12(5):6695–711.
- [59] Gai J, Tang L, Steward B. Plant localization and discrimination using 2d+ 3d computer vision for robotic intra-row weed control. In: 2016 ASABE annual international meeting. American Society of Agricultural and Biological Engineers; 2016, p. 1.
- [60] Sonka MHVBR. Image processing, analysis and machine vision. London: Chapman and Hall; 1993.
- [61] Mohammed Amean Z. Automatic plant features recognition using stereo vision for crop monitoring (Ph.D. thesis), University of Southern Queensland; 2017.
- [62] Bjurstrøm H, Svensson J. Assessment of grapevine vigour using image processing (Master's thesis), 2002.
- [63] Sural S, Qian G, Pramanik S. Segmentation and histogram generation using the hsv color space for image retrieval. In: Image processing. 2002. Proceedings. 2002 international conference on. Vol. 2. IEEE; 2002, p. II.
- [64] Lim JS. Two-dimensional signal and image processing. Englewood Cliffs, NJ: Prentice Hall; 1990, p. 710, 1990.
- [65] Nelikanti A. Image enhancement using image fusion and image processing techniques. *COMPUUSOFT Int J Adv Comput Technol* 2014;3(10):1193–7.
- [66] Foley JD, Van Dam A, et al. Fundamentals of interactive computer graphics. Vol. 2. Reading, MA: Addison-Wesley; 1982.
- [67] Valliammal N, Geethalakshmi S. Automatic recognition system using preferential image segmentation for leaf and flower images. *Comput Sci Eng: Int J* 2011;1:13–25.
- [68] Cerutti G, Tougne L, Mille J, Vacavant A, Coquin D. Understanding leaves in natural images—a model-based approach for tree species identification. *Comput Vis Image Underst* 2013;117(10):1482–501.
- [69] Kadir A, Nugroho LE, Susanto A, Santosa PI. Leaf classification using shape, color, and texture features. *Int J Eng Trends Technol* 2013;2(1):225–30.
- [70] Jain R, Kasturi R, Schunck BG. Machine vision. Vol. 5. New York: McGraw-Hill; 1995.
- [71] Sobel I, Feldman G. A 3x3 isotropic gradient operator for image processing. In: A talk at the stanford artificial project in. 1968, p. 271–2.
- [72] Cannby J. A computational approach to edge detection. *IEEE Trans Pattern Anal Mach Intell* 1986;6:679–98.
- [73] Zhu W, Zeng N, Wang N, et al. Sensitivity, specificity, accuracy, associated confidence interval and roc analysis with practical sas implementations. In: NESUG proceedings: health care and life sciences. Baltimore, Maryland; 2010. 19.
- [74] Liu S, Cossell S, Tang J, Dunn G, Whitty M. A computer vision system for early stage grape yield estimation based on shoot detection. *Comput Electron Agric* 2017;137:88–101.
- [75] Bradski G, Kaehler A. Learning OpenCV: Computer vision with the OpenCV library. O'Reilly Media, Inc; 2008.
- [76] Yun T, Chen B, Li W, Sun Y, Xue L. Using point cloud data for tree organ classification and real leaf surface construction. *Bulg Chem Commun* 2017;49(1):288–96.
- [77] Li Y, Su Y, Hu T, Xu G, Guo Q. Retrieving 2-d leaf angle distributions for deciduous trees from terrestrial laser scanner data. *IEEE Trans Geosci Remote Sens* 2018b;56(8):4945–55.
- [78] Xu Q, Cao L, Xue L, Chen B, An F, Yun T. Extraction of leaf biophysical attributes based on a computer graphic-based algorithm using terrestrial laser scanning data. *Remote Sens* 2019;11(1):15.